日本雪氷学会誌 雪 氷
78巻6号（2016年11月）365–382頁

論 文

Winter-spring transition of ground conditions over Alaska derived by airborne 6 GHz microwave and infrared observations

Nuerasimuguli ALIMASI[1,2]*, Hiroyuki ENOMOTO[1,3], Jessica CHERRY[4], Larry HINZMAN[4] and Takao KAMEDA[2]

Abstract

The rapid Arctic warming has been reported. Winter to spring shift of cryosphere is the key variables to be monitored related to warming mechanism. Satellite remote sensing is effective for observing cryospheric change from winter to spring. Although microwave observations with a frequency of 19 and 37 GHz have conventionally been used for the observation of snow covered areas, this study investigated use of the low-frequency 6 GHz band. To acquire information on the winter–spring transition of ground conditions in Alaska, flight observations of a forest, wetland and lake were performed using an airborne microwave radiometer. Infrared observation measures surface warming and low frequency microwave can observe inside of snow cover. This combination expands the information on spring snow conditions with warming and melting. The TB from the ground displayed little regional variation in the cold period. The variation increased when the spring snow melting season began. Surface temperature increased during the spring warming period, however, the ground below the snow cover remained cold. Flight and satellite microwave observations provided us with the monitoring capability for the spring warming over Alaska, and illustrate the early warming of lowland and late warming in the mountain areas around Fairbanks. Although inside of snow are still cold in the mountain area, significant warming in the forest, and warming in accelerating at wetland and lake in the low land.

Key words: Arctic, Alaska, cryosphere, spring, microwave

1. Introduction

The Arctic has recorded rapid warming at twice the speed of the global average (IPCC, 2013). This warming trend is largely derived from a temperature rise in the colder seasons. There has been reporting of the Arctic temperature rise, especially in winter season. Köhn and Royer (2012) showed that the winter temperature of the Arctic has been rising for the past 50 years, while ACIA (2005) reported that the temperature rise in winter is larger than the rise in summer in the high latitudes of the Northern Hemisphere. Arctic warming is evidenced in the rapid reduction of snow cover (Derksen and Brown, 2012). Arctic

1 National Institute of Polar Research, 10–3, Midori-cho, Tachikawa, Tokyo 190–8518
2 Kitami Institute of Technology, 165, Koen-cho, Kitami, Hokkaido 090–8507
3 Graduate University of Advanced Studies (SOKENDAI), 10–3, Midoricho, Tachikawa, Tokyo 190–8518
4 University of Alaska Fairbanks, 909 Koyukuk Drive, Fairbanks, AK 99775–7270, USA
* Corresponding author: alimasi.nipr@gmail.com

warming amplification has been studied to reveal the driving system of the rapid warming. Snow and ice cover reduction plays the key role for initiate spring time change (Yoshimori *et al.*, 2014). However, because there are few observation points in high latitudes, an increase in observational data is required to improve data reliability.

Remote sensing is an effective means of observing snow and ice phenomena in the Arctic region, particularly in the extensive, remote areas with extreme cold, where access is difficult. André *et al.* (2015) measured the surface temperature in the circumpolar Arctic using satellite microwave observational data. Taras *et al.* (2002) investigated the temperature of the snow cover and ground interface over the winter seasons along the Kuparuk River Basin in the North Slope of Alaska. They attempted to investigate the complex interactions between the ground and snow cover using 6 GHz microwave radiation. Even in a neighboring area of the North Slope bordering the Toolik River in northern Alaska, a large surface temperature difference was observed. This is not only a climatological air temperature contrast, but is also probably due to geographical and ground conditions.

Derksen *et al.* (2005) reported that snow depth is underestimated in forest and tundra, due to errors in microwave observation in forest areas. The influence of lakes, as well as the snow structure, produced errors in snow estimation (Lemmetyinen *et al.*, 2009; Derksen *et al.*, 2009). To improve the accuracy of snow cover observations by microwaves, measurements from beneath and within the snow cover should be evaluated. Microwave radiation is also influenced by the frozen ground. Tsutsui and Koike (2012) presupposed that the influence of biomass, snow grain size, and frozen ground are problems in the observation of snow depth by a microwave radiometer. They noted, as the ground under snow cover is frozen in cold regions, the boundary of the frozen soil beneath the snow should be considered.

Although snow detection has been carried out by detecting a non-scattering channel 36 GHz (Chang *et al.*, 1976), detection of deep accumulation was improved by using lower frequency channel (Kelly, 2009; JAXA, 2013)

Alimasi *et al.* (2016) conducted airborne microwave research over Alaska in the winter cold period, and incorporated microwave emissions from various ground components. The low frequency microwave band of 6 GHz was used to acquire information from inside the snow cover of forests and lakes in Alaska.

The present study expands the body of information for the winter-spring transition period. Differences in microwave radiation emissions between forests and various ground surface types were measured during the transition from winter to spring.

2. Arctic observations from winter to spring

2. 1 Inland Alaska in snow melting season

Olsson *et al.* (2003) divided the Arctic cold period into five stages, namely, early snow, early cold, deep cold, late cold, and thaw. Changes in snow and ice cover from winter to spring, corresponding to the late cold through to the thaw, are shifting in both seasonal cycles and long-term climate trends. The temperature was recorded at the University of Alaska, Fairbanks (UAF) campus, while Snow Telemetry (SNOTEL) data from the mountain area were also obtained for reference during the discussion.

Temperature changes from winter to spring at the UAF are shown in Fig. 1. The winter to spring temperature change occurs dramatically, and it starts snow melting season at the end of March. A low temperature of −30℃ was recorded in early March, which was followed by a temperature shift into the positive range, as the maximum temperature was 10℃ by the end of March.

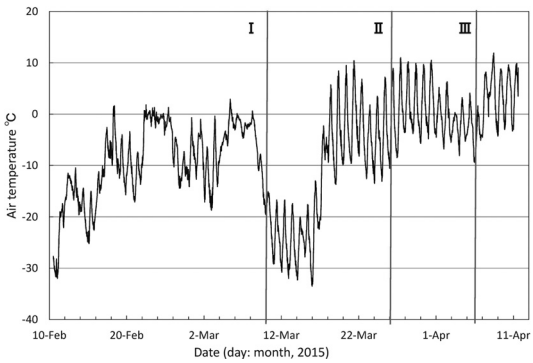

Fig. 1　Winter to spring temperature record at UAF site, Fairbanks. The flight observation was carried out on (I) March 10, (II) March 28 and (III) April 6, 2015.

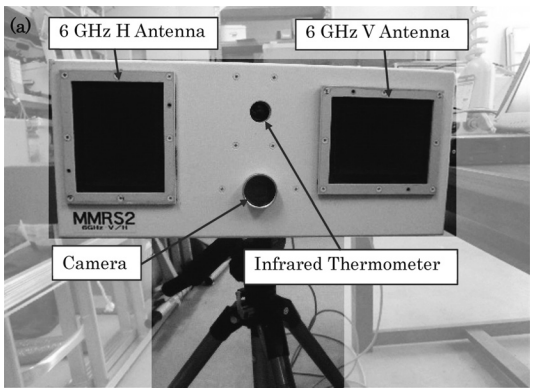

Fig. 2　Microwave radiometer MMRS2 used in this study. (a) Device construction, (b) the image shows field experiment at the Poker Flat Research Range (PFRR).

In order to observe cryospheric change occurring in this period, three observation flights were undertaken. The observation flights are marked on Fig. 1.

The first observation flight was performed on March 10, 2015. At this time, the temperature was about −20℃. The temperature fluctuated between −10 and 10℃ during observation flights II and III, which correspond to the transition period from winter to spring.

2. 2　Flight observations

A Cessna 182 light aircraft fitted with a microwave radiometer was used for the flight observations. The 6 GHz channel (6.925 GHz) was used as the observation frequency (Alimasi *et al.*, 2016; Tamura *et al.*, 2015). The microwave radiometer (MMRS2 Microwave/Millimeter-wave Radiometer System 2: Mitsubishi Electric Tokki System Corporation) was used is this study (Fig. 2a, b), and the specifications of the MMRS2 are given in Table 1.

The MMRS2 has a monitor camera and an infrared radiation thermometer. Microwave measurements were made for 150 ms, while the infrared measurements were made for an additional 400 ms. The measurements were recorded at 1 s intervals. The observation view angle of microwave radiometer (MMRS2) is 33° (Table 1). During observation, the flight altitude was maintained at 500 m above ground level. The ground footprint of each observation was approximately 300 m in diameter (IFOV). The infrared radiometer has the

Table 1　Specification of the MMRS2.

Item	Function
Frequancy (6 GHz - V/ 6 GHz - H)	6.925 GHz + 0.2 GHz
Observation brightness tepmerature (TB) range	3 - 1200 K
Accuracy	1 K Typ.@300 K
Observation viewing angle (TB)	33 deg
Power input (Body)	Battery/ DC 10 V - 17 V
Power input (heater)	DC 0 V - 27 V
Battery	15 V, 8.8 Ah
Battery charging time	About 9 hours
External output	LAN (Wireless/ wireline)
Observation Infrared temperature range	233 - 773 K
Observation viewing angle (Infrared)	2 deg
Camera	Visible
Operating environment	Temperature: -20℃ - +40℃ Humidity: Less than 80%
Dimension (Body)	380 mm x 500 mm x 165 mm (Width x Depth x Height)
Weight	About 12 kg

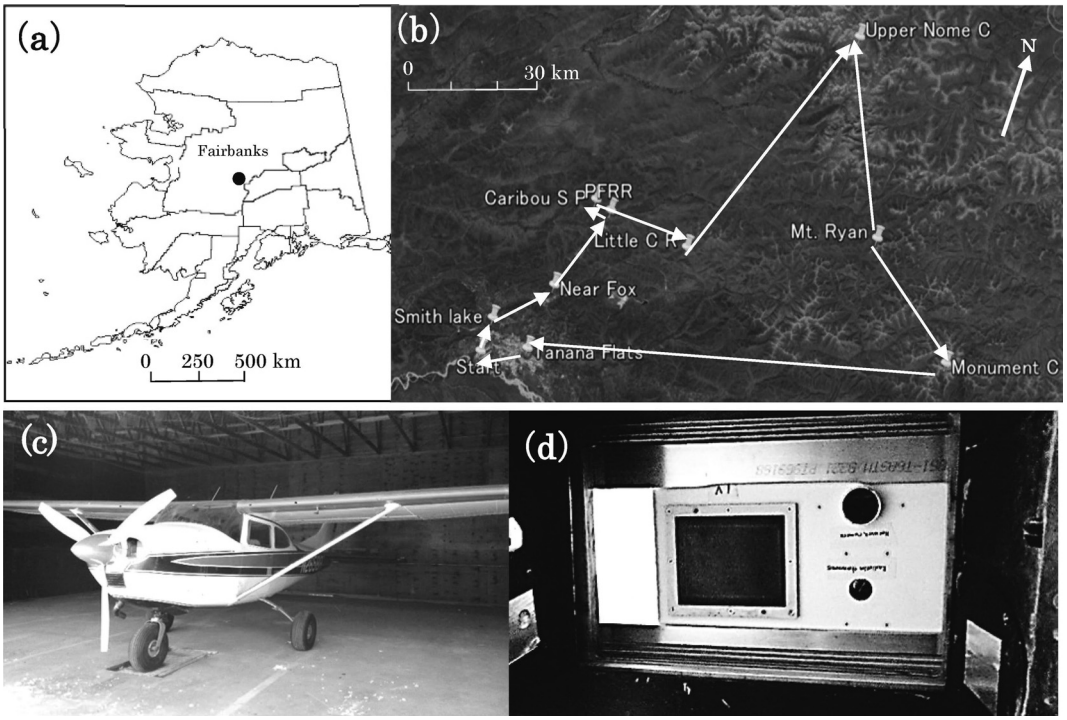

Fig. 3 Coordination of observation flight. (a) Map of Alaska and Fairbanks, (b) Flight observation route near Fairbanks, (c) Cessna 182 used for flight observation over Alaska, (d) MMRS2 set at the floor window of the airplane and view from below.

view angle 2° and approximately 14 m in diameter of observation area on the ground (IFOV). The microwave data and infrared data were integrated along the 308 m and 36 m when the flight speed was 200 km hr^{-1} (55 m s^{-1}).

The microwave radiometer was installed in a perpendicular direction (nadir) on the observation window in the cabin floor of the Cessna (Fig. 3 (c), 3 (d)). The data during the horizontal flight condition was used for analysis. Although polarization data were not obtained, these observations were useful to determine the difference in the microwave radiation emitted from various objects, and to determine seasonal change in the winter-spring transition period. A visual observation on the type and density of vegetation was also performed from the airplane.

Observation flight I lasted for approximately 3 h (from 11:40 to 14:40) on March 10, 2015 (local time). The actual observation period was approximately 2 hr for each flight. The temperature at the time of takeoff on March 10, 2015 was −19.5℃ (Fig. 1). The weathers during observation flights I (March 10) and II (March 28) were fine, whereas it was cloudy during observation flight III (April 6). The temperature was high during observation flight II. The conditions for each flight are listed in Table 2.

Observations were conducted over forest, lake, wetland and mountain areas around Fairbanks (Fig. 3 (a), 3 (b)). The flight route began in Fairbanks, then passed over Smith Lake, Little Chena River, Upper Nome Creek, Mt. Ryan, Monument Creek, and finally returned to Fairbanks. The data were summarized for the 13 targeted areas in Table 3.

2. 3 Extraction of satellite microwave data

Satellite microwave observation data over Alaska were obtained to see the large scale pat-

Table 2　Measurement condition of flight observation (Ⅰ, Ⅱ, Ⅲ).

Item	Ⅰ	Ⅱ	Ⅲ
Observation date and time	10 Mar 2015, 11:40-14:42	28 Mar 2015, 10:45-12:30	6 April 2015, 11:40-14:42
Observation area	Fairbanks, Alaska	Fairbanks, Alaska	Fairbanks, Alaska
Sampling interval (sec)	1	1	1
Air temperature (℃)	-19.5	-5.5	-2.3
Weather	Sunny	Sunny	Cloudy
Flight height	500 m	500 m	500 m
Frequancy	6.925 GHz	6.925 GHz	6.925 GHz
Observation angle	nadir	nadir	nadir

Table 3　Microwave brightness temperature (6 GHz) and surface temperature of the 13 ground types from observation I, II and III.

Flight	No.	1	2	3	4	5	6	7	8	9	10	11	12	13
	Type / Temperature	Dense black spruce	Dense white spruce	Dense birch	Black spruce	Sparse white spruce	Mixed spruce & birch	Scrub & Willows	Deep compacted snow	Bare ground snow	Marsh	Wetland	River side	Lake
Ⅰ	Brightness temperature TB_{6v} [K]	248 – 255	250 – 253	253 – 256	250 – 254	243 – 245	244 – 248	250 – 259	252 – 259	249 – 251	249 – 251	239 – 243	206 – 224	202 – 213
	Infrared temperature IR [K]	255 – 257	254 – 256	256 – 257	257 – 258	254 – 257	249 – 256	248 – 255	244 – 248	249 – 250	256 – 257	252 – 255	254	255
	Emssivity ε	.97 – .99	.98 – .99	.99 – 1.00	.97 – .98	.96 – .95	.98 – .97	1.01 – 1.02	1.03 – 1.04	1.00 – 1.00	.97 – .98	0.95	.81 – .88	.79 – .83
Ⅱ	Brightness temperature TB_{6v} [K]	261 – 262	260 – 261	262 – 264	251 – 260	251 – 259	254 – 257	254 – 261	256 – 257	252 – 259	259 – 265	242 – 252	230 – 238	238 – 255
	Infrared temperature IR [K]	276 – 279	277 – 279	275 – 279	276 – 279	275 – 279	276 – 277	272 – 276	271 – 272	271 – 276	275 – 278	274 – 277	275 – 276	272 – 277
	Emssivity ε	.94 – .93	.93 – .93	.95 – .94	.90 – .93	.91 – .92	.92 – .92	.93 – .94	.94 – .94	.92 – .93	.94 – .95	.88 – .90	.83 – .86	.87 – .92
Ⅲ	Brightness temperature TB_{6v} [K]	260 – 262	256 – 262	261 – 263	259 – 262	254 – 256	257 – 262	256 – 260	253 – 260	253 – 256	260 – 265	261 – 263	223 – 242	242 – 257
	Infrared temperature IR [K]	275 – 278	276 – 279	276 – 278	277 – 278	275 – 276	276 – 279	273 – 277	271 – 273	271 – 275	276 – 279	276	275 – 277	274 – 279
	Emssivity ε	.94 – .94	.92 – .93	.94 – .94	.93 – .94	.92 – .92	.93 – ,93	.93 – .93	.93 – .95	.93 – .93	.94 – .94	.94 – .95	.81 – .87	.88 – .92

tern of warming in spring. The Japan Aerospace Exploration Agency (JAXA) provides data from the microwave radiometer AMSR2 on board the Earth observation satellite Global Change Observation Mission-Water (GCOM-W). The data was obtained through Arctic Data archive System (ADS) established at National Institute of Polar Research (NIPR).

The 6 GHz vertical polarization (V) brightness temperature (TB) map over Alaska was obtained. In order to examine the detailed variation of microwave emissions, we extracted the TB data from each pixel along the airplane flight route. The size or horizontal resolution of each AMSR2 pixel used through ADS is 10 km × 10 km, and a total of 39 pixels were extracted, covering the full length of the route.

3. Results of observations

3. 1 Overview of all flight observation

The time series of the TB from the 6 GHz channel and the infrared radiation temperature obtained on the three observation flights are shown in Fig. 4. Differences in the surface temperatures are apparent in the data from the infrared radiation thermometer.

In flight I, the range in surface temperature was 250–260 K, while the range for flights II and III was 270–280 K. In flight I, the TB had a range of 200–290 K, which was centered around 255 K.

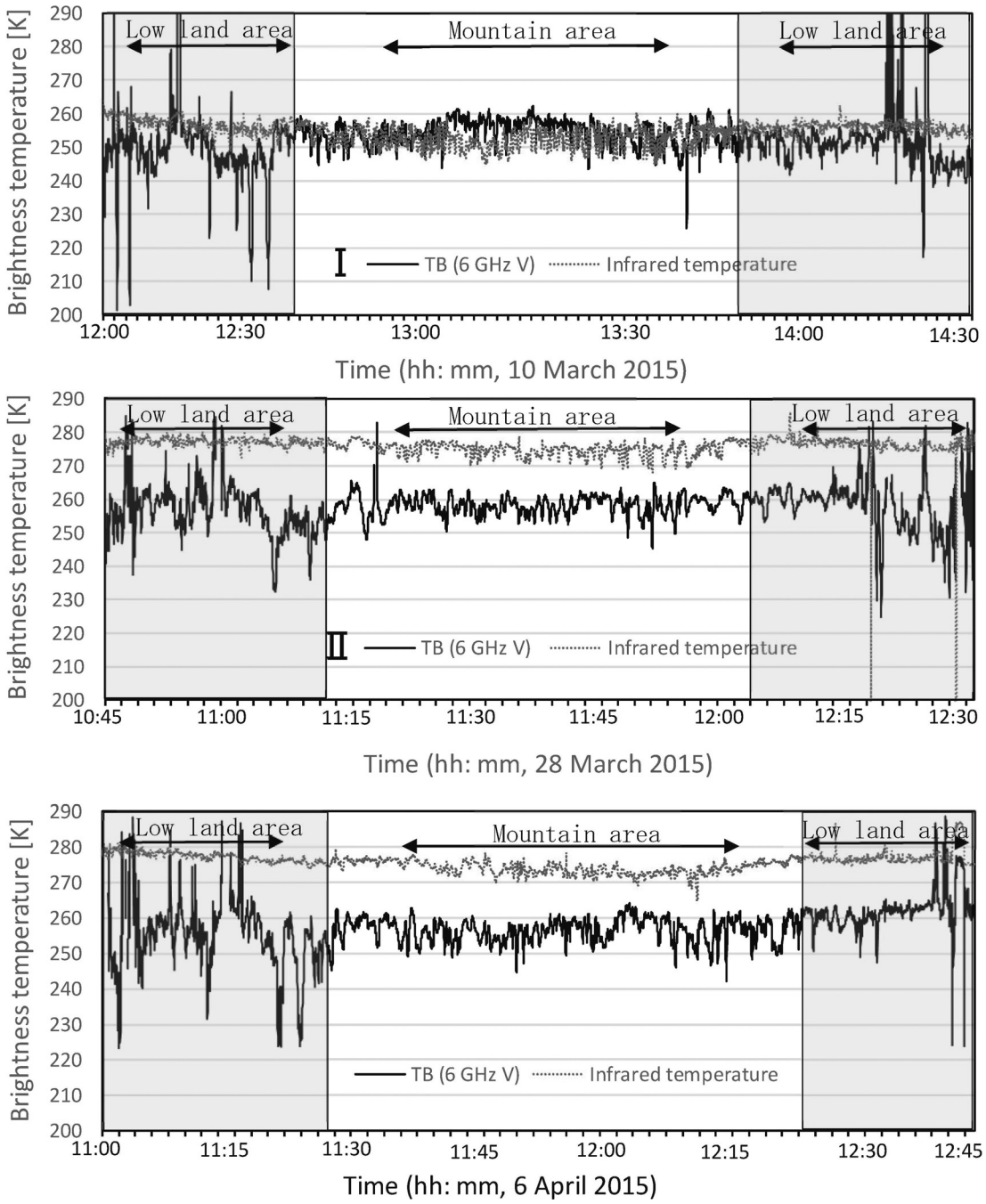

Fig. 4 Microwave and infrared data obtained from flight observation near Fairbanks on (I) March 10, (II) March 28 and (III) April 6, 2015. The solid line shows 6 GHz microwave brightness temperature, the dotted line shows infrared temperature.

In flight II, the TB had a range of 230–280 K, which was centered around 260 K. In Flight III, the TB had a range of 225–280 K, which was centered around 255 K. During flights II and III,

the surface temperature was high and snow melting had occurred. The surface temperature increased by approximately 20 K, while a TB increase of 5 K was obtained from flights I to II.

Large variations in the microwave radiation were apparent around Fairbanks city and the surrounding lowland area. The range of the TB was 200–260 K, whereas the range in surface temperature was smaller at 245–265 K. This area has many rivers, lakes, and wetlands, and the features of this area are described in Paragraph 3.2a.

In flight I, the TB values were lower than the values recorded by the infrared radiation thermometer during the beginning and final segments of the flight. However, the values of the TB became higher than the infrared radiation temperatures in the middle segment of the flight. The area with this inversion is located in the mountain area, the features of which are described in Paragraph 3.2b.

The range in TB of 245–255 K and surface temperature of 250–255 K were recorded over the forest area, the features of which are described in Paragraph 3.2c.

3.2 Distribution of microwave emissions

Thirteen different types of ground cover were selected from the images obtained from the three flights. The TB and surface temperature data were extracted for each ground cover type. Examples of typical surface cover types selected from aerial photographs are shown in Fig. 5. These are: 1) dense black spruce; 2) dense white spruce; 3) dense birch; 4) sparse black spruce; 5) sparse white spruce; 6) mixed spruce and birch; 7) scrub and willows; 8) deep compacted snow; 9) bare ground snow; 10) marsh; 11) wetland; 12) riverbank; and 13) lake.

The features of several specific cover types are summarized below.

8) Deep compacted snow (deep hardened snow in mountain areas): snow that has remained in place for a long time, with a light cover of fresh snow transported by the wind. The snow is compressed over time. With further snowfall, the existing snow becomes hardened further, and this process is repeated (No. 8 in Fig. 5).

9) Bare ground snow (snow cover on a field): fields with uneven snow cover across a wide area, which is influenced by fresh snowfalls and wind-blown snow, but generally has little snow coverage (No. 9 in Fig. 5).

10) Marsh (a marshy location, a swamp): humid or wet area containing little grass (No. 10 in Fig. 5).

11) Wetland (a marshland, a swamp): geographical feature, where lowlands are periodically flooded under the influence of a river or the sea (No. 11 in Fig. 5).

A scatter chart of infrared radiation temperature against TB is shown in Fig. 6. Six characteristic groups (A–F) were identified from the ground covering components. and are as follows: A) compacted snow in a mountain area; B) snowy field in a lowland area; C) dense forest; D) sparse forest; E) wetland and marsh; and F) lake and riverbank. The emissivity ε of the microwaves was calculated as:

$$\varepsilon = \mathrm{TB\,6\,GHz/IR}. \quad (1)$$

The IR observes the surface, 6 GHz TB is integrating emission through snow layers. Although targeting spaces are different, the equation (1) is used conditionally a measure of snow condition. The data are distributed in the zone of emissivity $\varepsilon = 0.8$–1.0. Surface temperature increased by approximately 20 K from flights I to II, and shows that surface temperature exceeded the melting point of snow. The TB increased by 5 K on average. The data scatter from flight II and III are overlapped across most parts of Fig. 6. Table 3 shows a summary of the observed values for the 13 ground types obtained from the three observation flights.

The following paragraphs summarize the evidence from the observations.

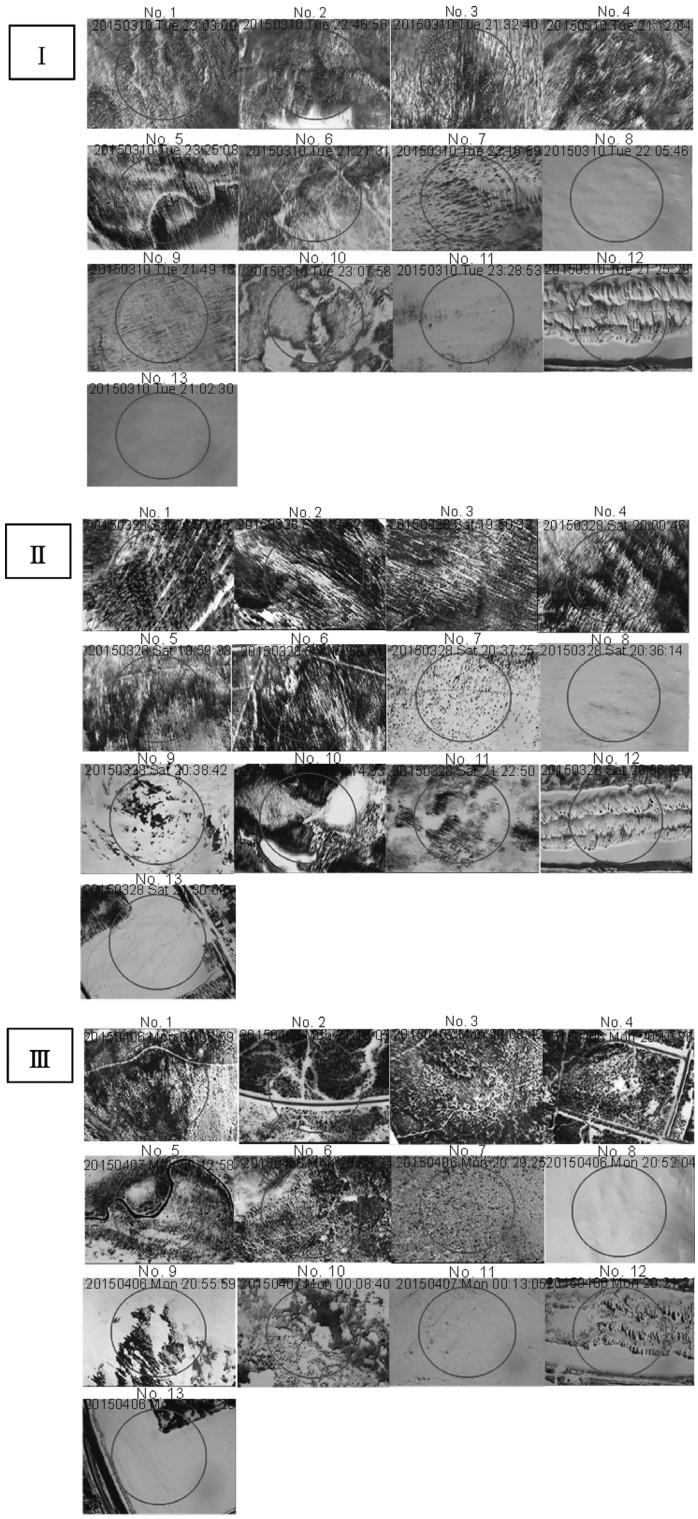

Fig. 5 Example of surface condition (No. 1～13) taken from the monitor camera of MMRS2. The circle in the image indicate field of view of microwave radiometer.

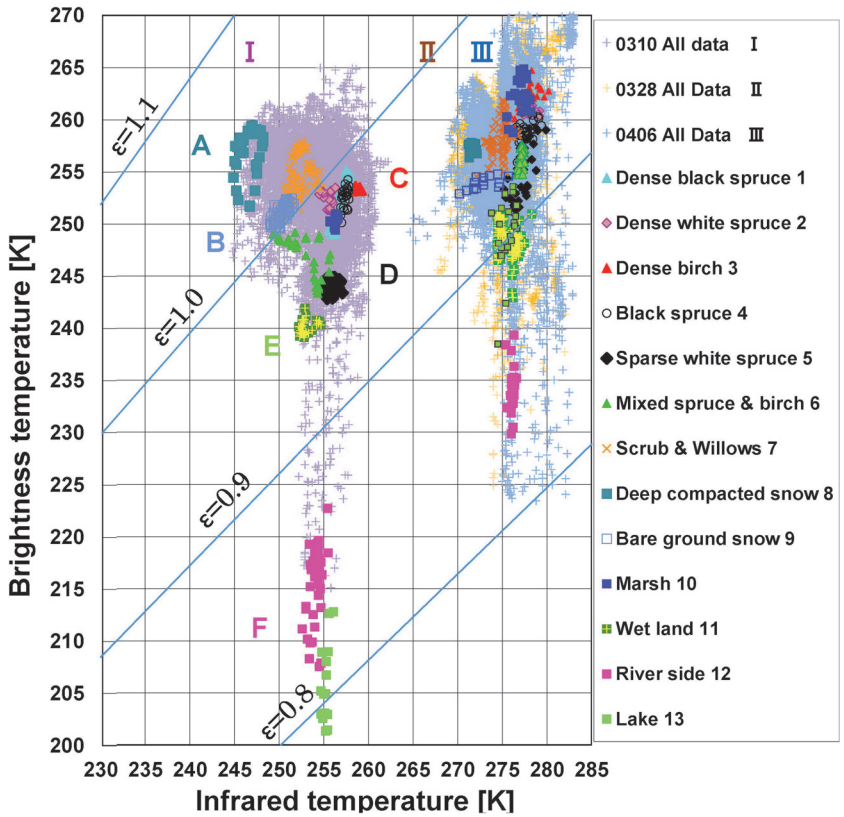

Fig. 6　Brightness temperature of 6 GHz microwave and infrared temperature from flight observations I, II and III. A) Compacted snow in a mountain area; B) snowy field in a lowland area; C) dense forest; D) sparse forest; E) wetland and marsh; F) lake and riverbank.

3. 2a.　Observation of a river and lake (E and F in Fig. 6)

There was an area along a river and lake where the TB decreased to 200 K in flight I. The lake was frozen at the time of the observations, and a visible image of the surface indicated snow cover. Although the snow covered, frozen lake was not distinguishable from a snowy field on land on the basis of color and surface temperature, a large difference was apparent from the TB at 6 GHz. The TB of marsh and swamp was 250 K, the TB of wetland was close to 240 K, while the riverbank of the Chena River had a TB range of 205–220 K. It is known that this area contains numerous puddles, and TB from these areas are low.

As the temperature rose from flights I to II, the TBs of the lake and riverbank increased from 202–228 K to 232–255 K, respectively, in the corresponding observations. Although the absolute values of these TBs are still low, the TBs are increasing.

3. 2b.　Snow cover on a mountain and bare ground (Fig. 6 A, B)

In Fig. 6, area A corresponds to compacted snow on a mountain, whereas area B corresponds to a snowy field in the lowlands. Area A is a snow covered region around Mt. Ryan (altitude: 3,481 ft/1,061 m), and wind packed snow cover was observed from the airplane.

The surface temperature was low in flight I, and the TB observed by the 6 GHz microwave radiometer was expected to reflect the tempera-

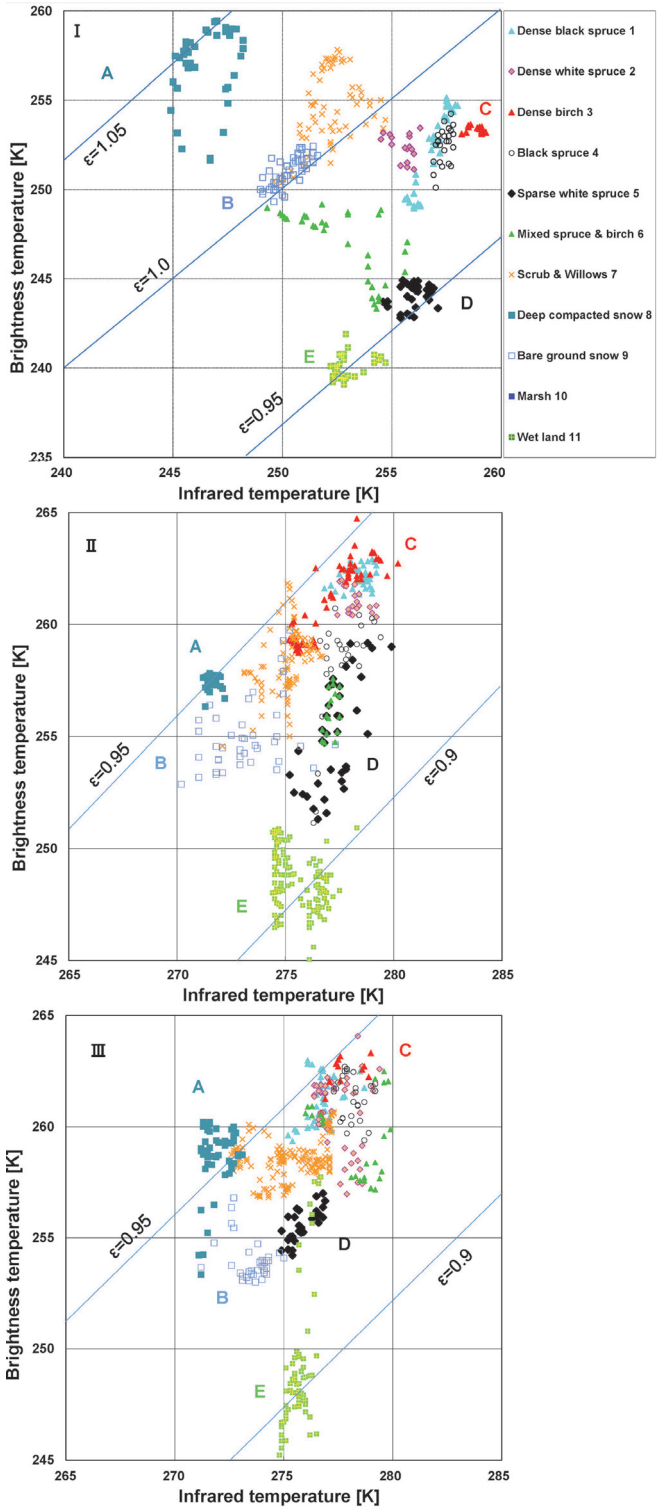

Fig. 7 Detailed map of brightness temperature of 6 GHz microwave and infrared temperature from flight observations I, II and III.

ture within or at the bottom of the snow cover. The surface temperature of this area increased by as much as 25 K from 248 K to 273 K between flights I and II, while the TB was largely unchanged. Then, the emissivity decreased to 0.94 in flight II.

The surface temperature was high, and the TB was low, over the snow cover of area B, which corresponds to lowland with less vegetation visible (bare ground snow). Areas with little snow cover and exposed ground were confirmed by airplane observations. Bare ground snow has larger emissivity compared to forest areas during the cold period (flight I).

3. 2c. Observation of forest areas

Fig. 7 shows the enlarged view of surface temperature and TB from groups A–E. Although the temperature ranges of each group were different, their relative distribution can be evaluated from these values.

There were common features observed in the three flights, despite flight I being made in a colder period, whereas flights II and III were made in a warmer period. A higher TB was apparent in the forest region than in other regions, and the surface temperature increased from 250–260 K in flight I to 273–280 K in flights II and III. The forest areas (No. 1–7) exhibited emissivity values between $\varepsilon = 0.95$ and 1.0 in flight I, but were between $\varepsilon = 0.9$ and 0.95 in flights II and III.

The surface temperature and TB values of scrub and willow area (No. 7) were scattered near those of snow cover on bare ground (No. 9). This area had large patches without vegetation, and was influenced by radiation from the snow surface. These results are summarized in Table 4.

Table 4 Summary of 6 GHz microwave signals from forest.

Tree type	Black spruce	White spruce	Birch	Scrub & Willows
Features	T_B is high or middle in the dense forest	T_B is a low in the dense and sparse forest	T_B high in the dense forest	T_B is affected by the back-ground snow

3. 3 Satellite observation

Satellite microwave observation data over Alaska and surrounding regions are shown in Fig. 8. The TB of 6 GHz shows warming over all of Alaska from March to April. There are slight gradients in the 6 GHz TB from the higher TB in the south to the lower TB in the north, and interestingly a warm band in the central part of Alaska, which includes Fairbanks. Comparison of the 6 GHz data with 36 GHz data, shows that the cold conditions are similar during flight I. However, compared to the 36 GHz data, there is remarkable contrast between the warm south and the cold north in the 6 GHz data from flights II and III. There is a remarkable contrast over Fairbanks, and this area exhibits distinct TB hotspots.

The satellite data corresponding to the flight observation area are shown in Fig. 9, which shows the microwave radiation distribution around the flight route. The radiation distribution showed only slight regional variation during flight I, with very similar TB values exhibited, except for slightly higher values in the mountain region around Mt. Ryan.

However, during flight II, there were regional differences in TB, except for the Mt. Ryan area. The lowlands and wetland around Fairbanks and the forest area had high TB values during flights II and III. The difference in TB values between mountain and lowland areas became apparent, whilst this difference is dramatic with the 36 GHz data.

The satellite TB data was extracted from a total of 39 pixels that cover the flight route, and are overlain on the route in Fig. 10. Each pixel size is 10 km × 10 km. The pixel or sample

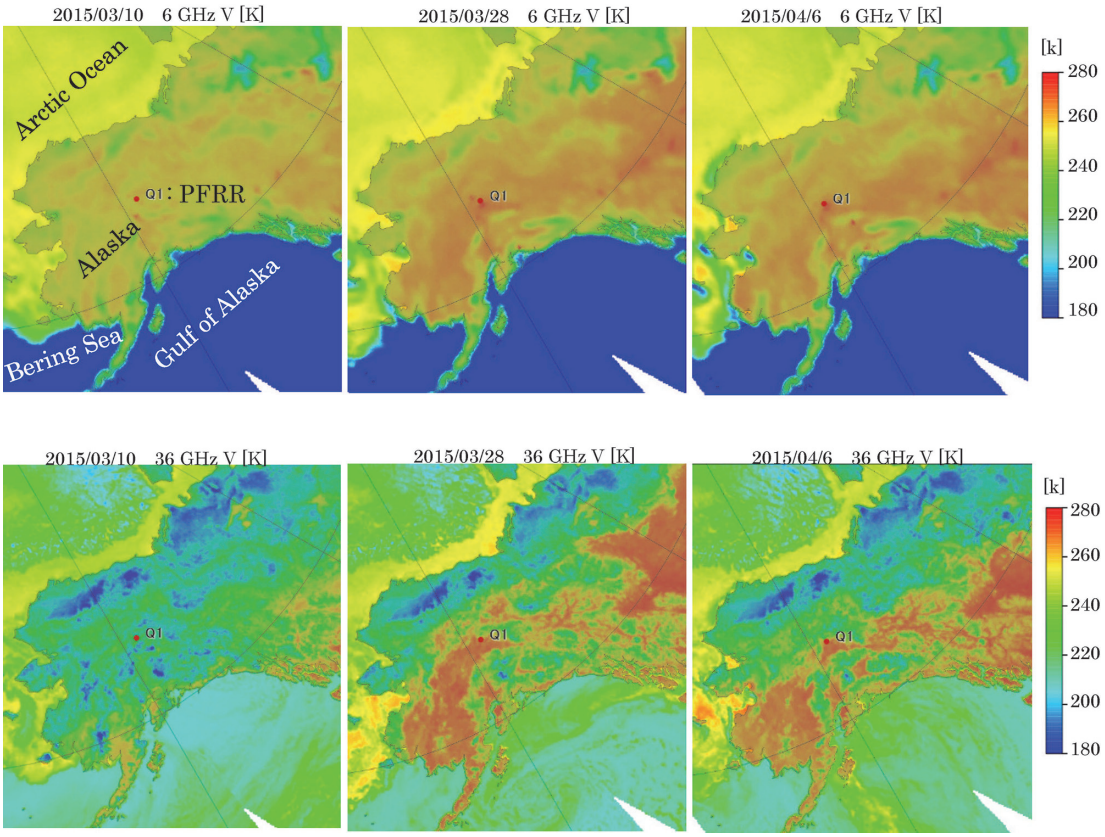

Fig. 8 Brightness temperature map for Alaska and surrounding regions at the observation I, II and III, obtained from GCOM-W AMSR2 6 GHz V and 36 GHz V. (Data: JAXA GCOM-W project, Projection: ADS.).

numbers 0–12 correspond to data from lowland and forest areas, 13–30 are from the mountain area, and 31–39 are from the lowland area.

The temporal changes in the TB were small in the mountain area, but were large in the lowland area. Furthermore, the regional differences in the TB were small during flight I, with a range in the differences of less than 5 K.

4. Discussion

4. 1 Winter-spring transition over Alaska

The flight observations in the present study captured TB signals from the winter to spring transition of snow covered areas. Three observation flights were carried out on cold and warm days in the winter-spring transition period. The flight route covered lowland and mountain areas. These observations provide unique information from the surface and within and beneath the snowpack of a snow covered region in Alaska.

The observations of surface temperature showed large increases of as much as 20 K in almost all areas in flights I to II. On the other hand, the TB of 6 GHz showed consistently low values during the cold period. Then, the TB increased during the warm period, and showed regional variations, especially differences between lowland and mountain areas. The largest increases were observed in wetland and frozen lake surfaces, with 30–60 K increases in TB, followed by forest areas with 10 K, and mountain areas with 5 K.

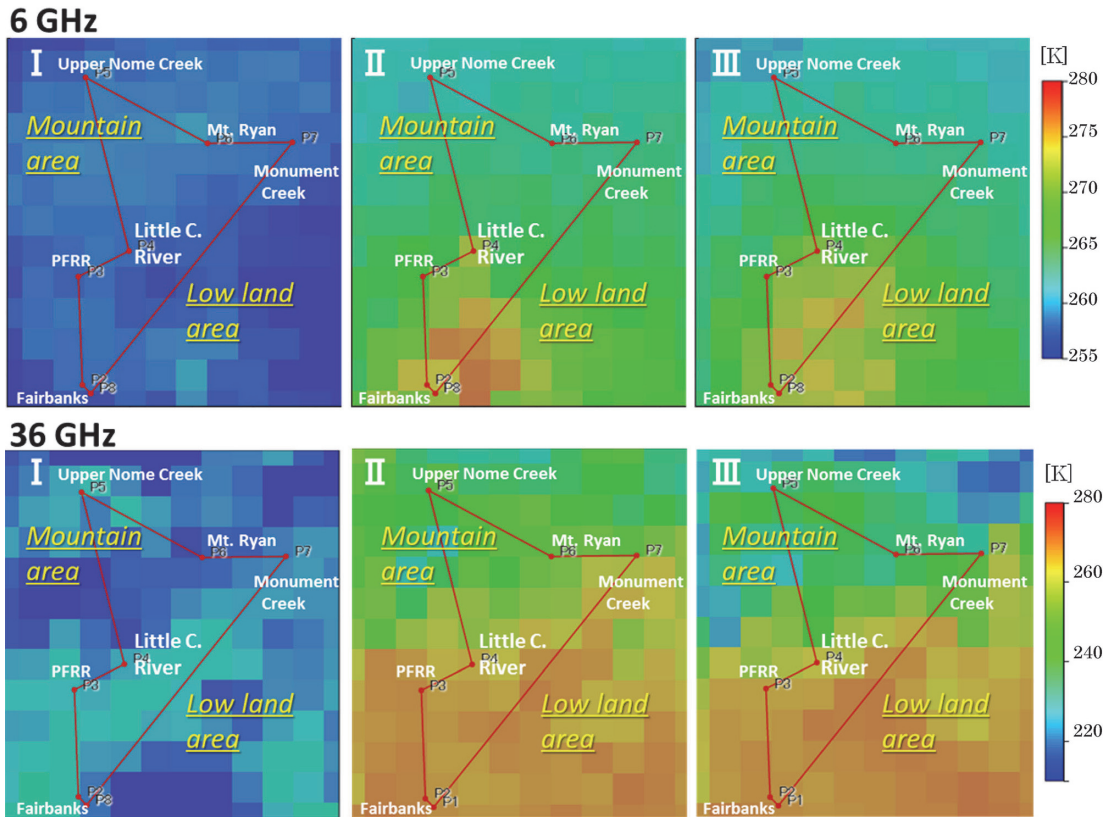

Fig. 9　Brightness temperature map for Fairbanks circumstances at the observation I, II and III, obtained from GCOM-W AMSR2 6 GHz V and 36 GHz V. Data pixel is 10 km × 10 km. The flight route is indicated on the image.（Data: JAXA GCOM-W, Projection: ADS.).

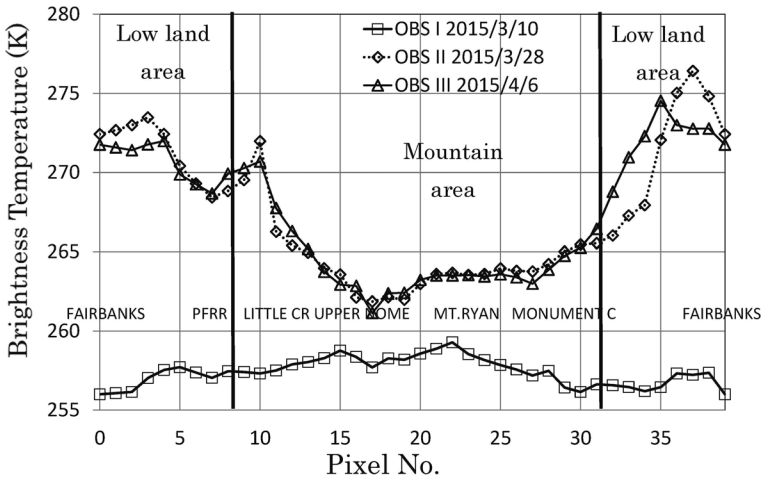

Fig. 10　Microwave brightness temperature profiles along the flight route at the observation I, II and III. Data was sampled by pixels of 10 km × 10 km. (Data: JAXA GCOM-W AMSR2 6 GHz V, data extraction: ADS.).

Table 5 Comparison of satellite and flight observation of 6 GHz around Fairbanks.

Obs. / Date / Data	Ⅰ March 10	Ⅱ March 28	Ⅲ April
Satellite Obs. Range [K]	255 – 259 4	262 – 276 14	261 – 275 14
Flight Obs. Range [K]	202 – 262 60	232 – 265 33	222 – 265 43

4. 2 Horizontal extent of spring warming

A drawback of remote microwave observation is that the spatial resolution is low, and because features occur on various spatial scales, an optimum scale should be considered to interpolate the data (Sturm and Benson, 2004). Evidence of the causes of fine scale variation would be useful when considering heterogeneous variation, and should be considered when interpreting the results of satellite observations at the subpixel level.

The Arctic contains a large number of lakes, and to observe areas where forest and lake cover is intermingled, requires an examination of mixtures of these features. In satellite microwave observation, a single observation data point (i.e., pixel) may contain many lakes that cannot be distinguished separately. During winter when the lakes freeze over, low TB values are maintained even if the lakes are covered with snow (Alimasi *et al.*, 2016).

The range of satellite and airborne flight TB of 6 GHz around Fairbanks are summarized in Table 5. The flight observations could distinguish the differences in the vegetation, rivers, lakes and wetlands (Fig. 7). Flight observations recorded a wide range of 60 K as a maximum, during flight I. This is due to the lower extremes of TB from lake and wetland observable by flight observation. In contrast, satellite observations showed only a 4 K range.

As the temperature rise began in spring, the satellite observations show wider variation (14 K), due to differences between lowland and mountain areas. As the flight observations have less variation in flights II and III, the flight and satellite observation ranges begin to approach each other. This is due to different rates of warming in lowland and mountain areas in spring.

Although it was not possible to distinguish detailed surface components in the satellite observations, difference between lowlands and mountain areas could be determined from data extracted from the satellite measurements (Figs. 8 and 9).

4. 3 Surface and subsurface conditions

The observation flights measured the surface temperature and microwave emission of 6 GHz, which indicates bottom of snow cover conditions. On the other hand, satellite observations at 36 GHz and 6 GHz observed surface and bottom of snow cover conditions.

The advantage of low frequency microwave is the penetration through snow cover. The TB values were relatively large in the mountain regions in flight I. This corresponds to the central portion of flight I in Fig. 2, and the area with compacted snow (A) in Figs. 6 and 7. Thus, this signature can be presumed to be microwave radiation from the ground surface under snow cover. The snow cover data for Mt. Ryan was acquired from neighboring Snow Telemetry (SNOTEL) observational data (Fig. 11). This provided the annual maximum snow depth at the time of flight I, which was 89 cm. Thus, the microwave radiation from beneath the snow cover area had been observed. SNOTEL sites also measure the air and ground temperature. The ground temperature was around 0℃. Irrespective of the low temperature, the conditions at the

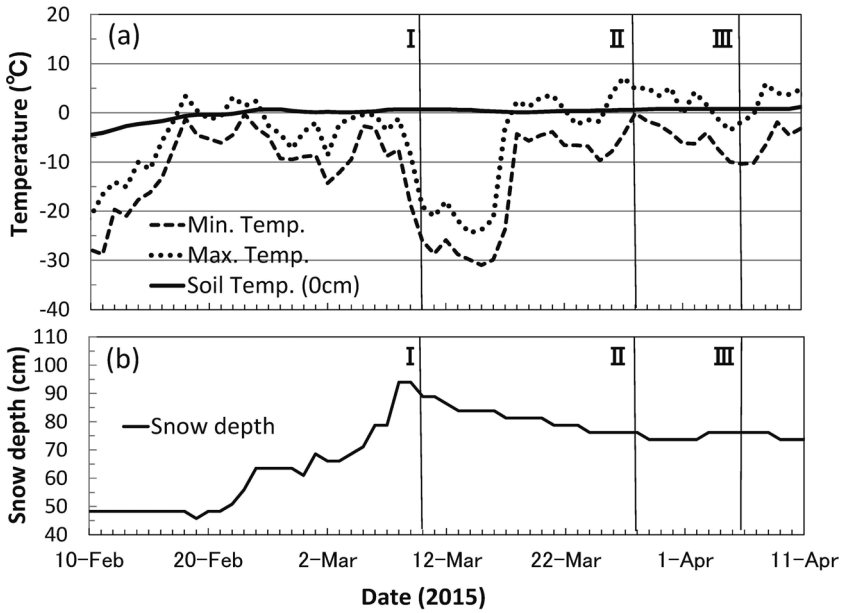

Fig. 11　Snow Telemetry (SNOTEL) observation data at Mt. Ryan, Alaska. (a) Air temperature and soil temperature (0 cm), (b) snow depth.

bottom of the snow layer after snowfall could be detected. The temperature gradient in the snow was reversed from flight I to II, due to surface warming of the snow. This is evidence of the winter to spring transition in the snow covered region, insofar as the microwave observations are detecting these changes.

Observations using low-frequency band can determine the state of the ground surface under snow cover. Tsutsui *et al.* (2010) discussed microwave emissions due to ground freezing under snow cover, and used the ratio between the 6 GHz and 19 GHz readings to determine this boundary. High values at 6 GHz were shown to reflect the frozen soil layer, and the condition of

$$TB\,6\,V/TB\,19\,V > 1 \qquad (2),$$

was used as an index. The investigation of snow cover using 6 GHz radiation can determine the conditions within the snow cover or on the ground beneath the snow cover. Tsutsui and Koike (2012) evaluated the soil under snow cover using 6 GHz radiation. In high latitudes, due to the presence of permafrost, the ground under snow cover was frozen. In a snow-covered area, microwave radiation is high, usually in the order of $6 > 18 > 36$ GHz, thus, the emissivity ε was set to $\varepsilon 6 > \varepsilon 18 > \varepsilon 36$. This can result in the observation of higher TB of 6 GHz.

The equation (2) is useful to survey soil condition under snow. This condition was developed at shallow snow and simple ground region. This will be useful if improved for the use in the forest region (*e.g.* Alaska).

Table 6 summarizes the surface and within, or bottom conditions of, snow cover expected from satellite 36 and 6 GHz observations (Fig. 9) and flight 6 GHz observations (Fig. 4). This can be presumed to be microwave radiation from the ground surface beneath the snow cover during the transition period from winter to spring.

For snow observation in forest areas, not only areal but volumetric application of the data was investigated. Langlois *et al.* (2011) determined that the influence of the trunk (stem volume) of a forest was significant in microwave observations.

Table 6 Surface and inside conditions of mountain and lowland, expected from microwave observations.

Obs. / Date / Area	Ⅰ March 10		Ⅱ March 28		Ⅲ April 6	
Low land & Forest	Surface	−	Surface	+	Surface	+
	Inside	− − −	Inside	+	Inside	+
Mountain area	Surface	− −	Surface	+ +	Surface	+ +
	Inside	− −	Inside	+ + +	Inside	+ + +

The 6 GHz microwave data is expected to be useful in evaluating the condition of the forest for trunk density information. They showed emissions of 6 GHz microwave radiation was high in a dense forest region, which the results of the present study also confirm. From our observations, the TB from scrub and willow was lower, as this area had large patches without vegetation, and thus was more strongly influenced by radiation from the snow cover.

Paloscia and Pampaloni (1988) investigated the microwave emission from vegetation using 10 GHz band. Recently using lower frequency of microwave, forest evaluation by microwave emissions alone (Santi *et al.*, 2012; Roy *et al.*, 2014) will be useful for procedure of snow observation flow applicable to forest regions. If the microwave radiation from vegetation can be quantified, it can function as a vegetation index. These approaches are useful not only reduction of noise by vegetation but also indication of vegetation, through the evaluation of vegetation water content.

5. Conclusion

This study investigated effective observation on the winter-spring transition of the Arctic cryosphere. Flight observations of various snow covered regions around Fairbanks, Alaska were performed using a portable microwave radiometer with a frequency of 6 GHz and infrared thermometer. Winter-spring seasonal changes in the microwave emissions from the ground can be summarized below.

- There is a large distribution of wetland and lakes in the Arctic permafrost region. Despite the snow cover, the airborne microwave radiometer detected frozen lakes by the significant decline in the TB of 6 GHz over the lake.

- Forest is the important area to be evaluated for snow observation by remote sensing. The TBs from forest area were incorporated. The TB values were high in the dense forests.

- Although the high mountain area contained cold surfaces as observed by infrared, the TB of 6 GHz was relatively high and stable over time.

- The regional differences in microwave radiation increased when the spring snow melting period began, except in the mountain area. At the time of the spring snow melting, the increases in the TB in the forest and damp area were significant.

- The flight observations evaluated 6 GHz TBs from various circumstances, so that influences of each component of satellite observation pixels are elucidated.

The 6 GHz microwave observation combined with infrared observation, as with its application to snow, forest, wetland and frozen ground, can be used for research of Arctic circumstances and useful to their cryospheric monitoring.

Acknowledgement

We are indebted to Mr. Craig Kenmonth, Dr. Hajo Eicken, Dr. Go Iwahana and Dr. Andy Mahoney and many IARC/UAF researchers. The comments from anonymous reviowers are very useful. We used GCOM-W/AMSR2 data of JAXA.

The data processes are supported by the Arctic Data archive System (ADS) in National Institute of Polar Research (NIPR). The author (NA) thanks the young dispatch support by the Japan Consortium for Arctic Environmental Research. This research is done as a part of a GRENE Arctic research project and Arctic project of NIPR.

References

ACIA, 2005: *Arctic Climate Impact Assessment*, Cambridge University press, NY, 1042 pp.

Alimasi, N., H. Enomoto, J. Cherry, L. Hinzman, T. Kameda, K. Sugiura and M. Hori, 2016: Airborne 6 GHz passive microwave observation of winter ground conditions in Alaska, *Seppyo (Snow and Ice)*, **78** (4), 185–203. (in Japanese)

André, C., C. Ottlé, A. Royer and F. Maignan, 2015: Land Surface Temperature Retrieval over circumpolar Arctic using SSM/I-SSMIS and MODIS Data, *Rem. Sens. Enviro.*, **162**, 1–10.

Bekryaev, R. V., I. V. Polyakov and V. A. Alexeev, 2010: Role of polar amplification in long-term surface air temperature variations and modern Arctic warming. *Journal of Climate*, **23**, 3888–3906.

Chang, A. T. C., P. Gloersen, T. Schmugge, T. T. Wilheit and H. J. Zwally, 1976: Microwave emission from snow and glacier ice, *J. Glaciol.*, **16**, 23–39.

Derksen, C. and R. Brown, 2012: Spring snow cover extent reductions in the 2008–2012 period exceeding climate model projections, *Geophys. Res. Lett.*, **39** (19), L19504, doi:10.1029/2012GL053387

Derksen, C., A. Walker and B. Goodison, 2005: Evaluation of passive microwave snow water equivalent retrievals across the boreal forest/tundra transition of western Canada, *Rem. Sens. Enviro.*, **96** (3/4), 315–327.

Derksen, C., M. Sturm, G. E. Liston, J. Holmgren, H. Huntington, A. Silis and D. Solie, 2009: Northwest Territories and Nunavut Snow Characteristics from a Subarctic Traverse: Implications for Passive Microwave Remote Sensing, *Journal of Hydrometeorology*, **10**, 448–463.

IPCC, 2013: *Climate Change 2013, The Physical Science Basis*. Contribution of Working Group I to the Fifth Assessment Report of the Intergovernmental Panel on Climate Change, edited by T. F. Stocker, D. Qin, G.-K. Plattner, M. Tignor, S. K. Allen, J. Boschung, A. Nauels, Y. Xia, V. Bex and P. M. Midgley, Cambridge University Press, NY, 1535 pp.

JAXA EORC, 2013: Algorithm description of GCOM-W1 AMSR2, *JAXA Technical Report*, NDX-1200015 A, 119.

Kelly, R., 2009: The AMSR-E snow depth algorithm: description and initial results, *Journal of the Remote Sensing Society of Japan*, **29** (1), 307–317.

Köhn, J. and A. Royer, 2012: Microwave brightness temperature as an indicator of near-surface air temperature over snow in Canadian northern regions, *International Journal of Remote Sensing*, **33** (4), 1126–1138. http://dx.doi.org/10.1080/ 01431161.2010.550643.

Langlois, A., A. Royer, F. Dupont, A. Roy, K. Goita and G. Picacard, 2011: Improved Corrections of Forest Effects on Passive Microwave Satellite Remote Sensing of Snow Over Boreal and Subarctic Regions, *IEEE Transactions On Geoscience And Remote Sensing*, **49** (10), 3824–3837.

Lemmetyinen, J., C. Derksen, J. Pulliainen, W. Strapp, P. Toose, A. Walker, S. Tauriainen, J. Pihlflyckt, J. P. Kärnä and M. T. Hallikainen, 2009: A comparison of airborne microwave brightness temperatures and snowpack properties across the boreal forests of Finland and western Canada, *IEEE Transactions On Geoscience And Remote Sensing*, **47** (3), 965–978.

Olsson, P. Q., M. Sturm, H. CH. Racine, E. V. Romanovsky and G. E. Liston, 2003: Five stages of the Alaskan Arctic cold season with Ecosystem implications, *Arctic, Antarctic, and Alpine Research*, **35**, 74–81.

Paloscia, S., and P. Pampaloni, 1988: Microwave polarization index for monitoring vegetation growth. IEEE Trans. *On Geoscience and Remote Sensing*, GE, **26** (5), 617–621.

Roy, A., A. Royer and R. Hall, 2014: Relationship between forest microwave transmissivity and structural parameters for the Canadian boreal forest, *IEEE Geoscience and Remote Sensing Letters*, **11** (10), 1802–1806.

Santi, E., S. Pettinato, S. Paloscia, P. Pampaloni, G. Macelloni and M. Brogioni, 2012: An algorithm for generating soil moisture and snow depth maps from microwave spaceborne radiometers: *Hydroalgo, Hydrology and Earth System Science Discussions*, **9**, 3851–3900.

Sturm, M. and C. Benson, 2004: Scales of spatial heterogeneity for perennial and seasonal snow layers, Snow Layer Heterogeneity, *Annals of Glaciology*, **38** (1), 253–260 (8).

Tamura, T., K.I. Ohshima, J.L. Lieser, T. Toyota, K. Tateyama, D. Nomura, K. Nakata, A.D. Fraser, P.W. Jansen, K.B. Newbery, R.A. Massom and S. Ushio, 2015: Helicopter-borne observations with portable microwave radiometer in the Southern Ocean and the Sea of Okhotsk, *Annals of Glaciology*, **56**, 436–444.

Taras, B., M. Sturm and G.E. Liston, 2002: Snow–ground interface temperatures in the Kuparuk River Basin, Arctic Alaska: measurements and model, *Journal of Hydrometeorology.*, **3**, 377–394.

Tsutsui, H., T. Koike, 2012: Development of snow retrieval algorithm using AMSE-E for the BJ ground based station on seasonally frozen ground at low altitude on the Tibetan plateau, *Journal of the Meteorological Society of Japan*, **90** (C), 99–112.

Tsutsui, H., Koike, T, Li, X., Jin, R., Lu, H., 2010: Application of the frozen soil layer into the micro wave radiative transfer model and improvement of the satellite retrieval algorithm for dry snow, *Annual Journal of Hydraulic Engineering*, **54**, 415–420 (in Japanese).

Yoshimori, M., M. Watanabe, A. Abe-Ouchi, H. Shiogama and T. Ogura, 2014: Relative contribution of feedback processes to Arctic amplification of temperature change in MIROC GCM, *Clim. Dyn.*, **42**, 1613–1630.

航空機搭載 6 GHz マイクロ波放射計と赤外線を用いたアラスカ地表面の冬から春への遷移観測

Nuerasimuguli ALIMASI[1,2*]，榎本浩之[1,3]，Jessica CHERRY[4]，Larry HINZMAN[4]，亀田貴雄[2]

[1] 国立極地研究所
〒190–8518 東京都立川市緑町 10–3
[2] 北見工業大学
〒090–8507 北海道北見市公園町 165 番地
[3] 総合研究大学院大学
〒190–8518 東京都立川市緑町 10–3
[4] アラスカ大学フェアバンクス校
909 Koyukuk Drive, Fairbanks, AK 99775–7270
* 連絡先：alimasi.nipr@gmail.com

要　旨

北極圏では急速な温暖化が報告されている．温暖化のメカニズムの研究では，冬から春にかけての雪氷圏の変化が注目されているが，衛星リモートセンシングは冬から春の雪氷圏観測の有効な手法である．これまで積雪域の観測には 37 GHz, 19 GHz のマイクロ波を使った観測が用いられてきたが，本研究では低周波の 6 GHz の利用を検討した．冬から春のアラスカの地表面の変化の観測のために，航空機搭載マイクロ波放射計によるアラスカの湖や湿地，森林地帯の観測を実施した．積雪の昇温が起こり，融解が始まる春の雪氷域では表面を観測する赤外線と内部を観測する低周波マイクロ波の組み合わせが有効である．積雪融解前は TB の地域差はほとんど見られなかったが，融解期の開始とともに違いが大きくなった．冬から春にかけて，赤外線が示す表面温度の上昇の一方で積雪底部はまだ低温状態にある．航空機と衛星観測により，アラスカの春の昇温の進行におけるフェアバンクス周辺の低地の速い昇温と山岳の昇温の遅れが観測出来た．また，山岳域では積雪内部の昇温の遅れ，低地では森林の顕著な昇温と湿地や凍結している湖での昇温の進行が観察できた．

キーワード：北極，アラスカ，雪氷圏，春季，マイクロ波

（2016 年 6 月 27 日受付，2016 年 9 月 10 日改稿受付，2016 年 10 月 6 日受理，討論期限 2017 年 5 月 15 日）